Bioresource Technology 102 (2011) 142–149

Contents lists available at ScienceDirect

Bioresource Technology

journal homepage: www.elsevier.com/locate/biortech

Modelling neutral lipid production by the microalga *Isochrysis* aff. *galbana* under nitrogen limitation

Francis Mairet [a,*], Olivier Bernard [a], Pierre Masci [a], Thomas Lacour [b], Antoine Sciandra [b]

[a] COMORE-INRIA, BP93, 06902 Sophia-Antipolis Cedex, France
[b] LOV, UMR 7093, BP28, 06234 Villefranche-sur-mer, France

ARTICLE INFO

Article history:
Received 24 March 2010
Received in revised form 25 June 2010
Accepted 29 June 2010
Available online 24 July 2010

Keywords:
Phytoplankton
Growth model
Nitrogen starvation
Neutral lipid
Biofuel

ABSTRACT

This article proposes a dynamical model of microalgal lipid production under nitrogen limitation. In this model, intracellular carbon is divided between a functional pool and two storage pools (sugars and neutral lipids). The various intracellular carbon flows between these pools lead to a complex dynamic with a strong discrepancy between synthesis and mobilization of neutral lipids. The model has been validated with experiments of *Isochrysis* aff. *galbana* (clone T-iso) culture under various nitrogen limitation conditions and under nitrogen starvation. The hysteresis behavior of the neutral lipid quota observed experimentally is accurately predicted.

1. Introduction

Some microalgal species are known both for their ability to synthesize and accumulate considerable amounts of lipids (Metting, 1996) and for their high growth rate. This potential has led some authors to consider that microalgae could be one of the main biofuel producers in the future (Huntley and Redalje, 2007; Chisti, 2007). These authors claimed that biodiesel productivities would be at least in a range of magnitude higher than terrestrial plants productivities. However, the conditions for neutral lipid accumulation (triacylglycerols are the best substrate to produce biodiesel) and for high growth rate are generally antagonistic. Nitrogen starvation increases the cell lipid content but at the same time strongly reduces the growth rate (Pruvost et al., 2009; Rodolfi et al., 2009; Sobczuk and Chisti, 2010). Lipid productivity, which is the outcome of these two factors, requires a trade-off between biomass production and oil content (Hsieh and Wu, 2009; Lv et al., 2010). Nitrogen-limited continuous cultures, which allow the control of the cell growth by maintaining a suboptimal nitrogen level (Falkowski and Raven, 2007), prevent the cells to become starved and to stop growing. Identifying a trade-off between neutral lipid accumulation and growth is therefore a key issue for optimizing biodiesel productivity.

The main objective of our work is to develop a dynamical model able to predict neutral lipid productivity under nitrogen stress in order to propose an optimization strategy. The model is developed on the basis of experiments carried out in various nitrogen conditions (replete, limitation and starvation) with the prymnesiophyceae *Isochrysis* aff. *galbana* (clone T-iso). The model complexity must result from a trade-off between realism, in order to accurately represent the key variables of the process, and simplicity so that it can be mathematically tractable and suitable for calibration and to solve optimal control problems (Bernard and Queinnec, 2008). The simplest model for describing growth of a population of microalgae limited by nitrogen is the Droop model (Droop, 1968, 1983). This model assumes that the growth rate depends on the intracellular concentration of nitrogen. More accurate models have been proposed to deal with the coupling between nitrogen and carbon assimilation in various light conditions (Geider et al., 1998; Faugeras et al., 2004; Pahlow, 2005; Ross and Geider, 2009), but none of them predict the lipid fraction. The model which is presented in this work is, to our knowledge, the first one dealing with neutral lipid production by microalgae.

The article is structured as follows: in Section 2, the experimental approach is presented and the model design and hypotheses are detailed. Then, we describe the model calibration procedure. In Section 3, we validate the model with experimental data of a *Isochrysis* aff. *galbana* culture, with various rates of nitrogen limitations. Finally, an analysis of the model behaviour is presented and a discussion about neutral lipid productivity concludes the article.

2. Methods

2.1. Experimental approach

Cultures of *Isochrysis* aff. *galbana* (clone T-iso, CCAP 927/14) were grown in 5 L cylindrical vessels at constant temperature

* Corresponding author. Tel.: +33 4 92 38 71 74; fax: +33 4 92 38 78 58.
E-mail address: francis.mairet@inria.fr (F. Mairet).

0960-8524/$ - see front matter © 2010 Elsevier Ltd. All rights reserved.
doi:10.1016/j.biortech.2010.06.138

(22.0 ± 0.1 °C), light (430 ± 30 μmol quanta m^{-2} s^{-1} in the centre of the culture vessel) and pH (maintained at 8.2 by automatic injection of CO_2). The experiment consists of imposing nitrogen limitation through a succession of dilution rates changes (1, 0.2, 0.4, 0.6, 0.8 and 1 d^{-1}). Each dilution rate was maintained until the steady state of the internal quota (which is slower than, e.g. cell density) was apparently reached. Two chemostats were run in parallel under identical conditions except for the final days: dilution was stopped to obtain a nitrogen starvation in photobioreactor A whereas a nitrogen limitation was imposed (with a low dilution rate) in photobioreactor B. The influent nitrogen concentration was modified to maintain biomass concentration in a reduced range and thus avoid any bias that would result from light change in the reactor. Fig. 1 presents the operating conditions. The first part of the experiment (from the beginning to day 18) was used for model calibration, the remaining set of data is kept for model validation.

Nitrate and nitrite concentrations were measured every 2 h with a Technicon Auto-analyzer coupled to an automated data-acquisition system. The concentrations of particulate carbon and nitrogen were determined every day on triplicate samples. Ten millilitres of culture were filtered onto glass-fiber filters (Whatman GF/C) precombusted at 500 °C for 12 h. Filters were kept at 60 °C before elemental analysis with a CHN analyzer (Perkin–Elmer 2400 Series II CHNS/O). Cell concentration and size distribution were automatically measured hourly with an optical particle counter using the principle of light blockage (Hiac/Royco, Pacific Scientific Instruments) and were used to compute biovolume. A correlation between biovolume and particulate carbon is used to convert the biovolume measurements into particulate carbon in order to have an hourly estimate of particulate carbon. Carbohydrate concentrations were determined in duplicate samples of 5 mL of culture filtered onto precombusted glass-fiber filters (Whatman GF/C). Total carbohydrate concentrations were analysed by the phenol method (Dubois et al., 1956). Total lipids were quantitatively extracted using the method of Bligh and Dyer (1959). After an initial extraction of the tissue with a monophasic mixture of chloroform:methanol:water (1:2:0.8, v/v), chloroform and water were added for phase separation. Lipids are present in the chloroform phase which is evaporated. All lipid extracts were stored at 80 °C until analysis. To avoid lipid auto-oxidation, a nitrogen atmosphere was maintained all the time. Separation of neutral and polar (glycolipids and phospholipids) lipids was achieved on a preparative scale by column chromatography on silica gel (Extract-Clean, Alltech). The neutral lipid fraction was eluted with six column volumes of chloroform, and then evaporated and weighted. Lipid and sugar measurements were converted in g[C] using the following conversion factors: 0.4 g[C] g DW^{-1} for carbohydrates and 0.76 g[C] g DW^{-1} for neutral lipids (Geider and Roche, 2002). For more details on the experiment protocol see Le Floc'h et al. (2002).

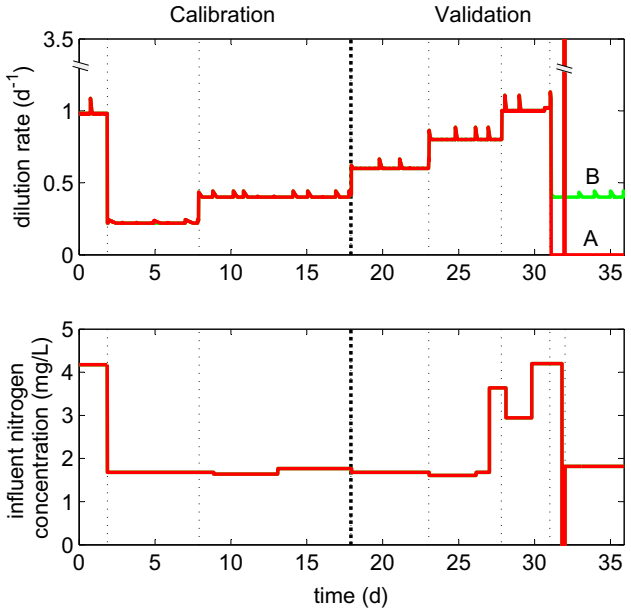

Fig. 1. Operating conditions for experiment with *Isochrysis* aff. *galbana*. Dilution rate variations impose various nitrogen limitations. At the end, in photobioreactor A dilution was stopped to obtain a nitrogen starvation whereas in photobioreactor B a nitrogen limitation was imposed with a low dilution rate.

2.2. Model design

The objective of the mathematical model is to support an optimization strategy and to guide the trade-off between growth and lipid accumulation. It must keep complexity at a minimal level to be mathematically tractable. We therefore limited the number of variables to the most important ones. We focus on the growth of microalgae, whose biomass, in terms of organic carbon, is denoted x. These microalgae are limited by an inorganic nitrogen source (nitrate, denoted s). In line with Ross and Geider (2009), we consider that organic carbon can be split into functional and storage pools. The functional compartment (f) includes the biosynthetic apparatus (proteins and nucleic acids) and the structural material (membranes mainly made of glycolipids and phospholipids). However, we add a new distinction: the storage pool is divided into a sugar reserve compartment (g) and a neutral lipid reserve compartment (l).

Nutrient uptake and biomass growth are known to be uncoupled processes for microalgae (Droop, 1983) leading thus to variations in the internal quota of nutrient.

Nutrient is taken up by the microalgae to make cellular nitrogen (n) at rate $\rho(s)$. This flux of nitrogen can be summarized in the following macroscopic reaction which represents the mass flux between the inorganic and organic compounds:

$$s \xrightarrow{\rho(s)x} n \tag{1}$$

The absorption rate $\rho(s)$ is taken as a Michaelis–Menten function:

$$\rho(s) = \rho_m \frac{s}{s + K_s} \tag{2}$$

with K_s the half-saturation constant for the substrate and ρ_m the maximum uptake rate.

In line with the Droop modelling approach, we consider that the specific growth rate μ, i.e. the net incorporation of CO_2 is an increasing function of the internal quota of nutrient ($q_n = \frac{n}{x}$). We assume that inorganic carbon is first incorporated in the pool of sugars g:

$$CO_2 \xrightarrow{\mu(q_n)x} g \tag{3}$$

This macroscopic reaction summarizes the set of reactions that occur in the dark phase of photosynthesis, and that lead, through the Calvin cycle to the production of carbohydrates such as glucose 6-phosphate (Falkowski and Raven, 2007). The mathematical expression for the specific growth rate μ is chosen using Droop model (Droop, 1968):

$$\mu(q_n) = \bar{\mu}\left(1 - \frac{Q_0}{q_n}\right) \tag{4}$$

where $\bar{\mu}$ and Q_0 represent the theoretical maximum growth rate and the minimum nitrogen quota allowing growth, respectively.

The sugar compartment g is then used in a second stage to synthesize the functional elements of the biomass f:

$$g \xrightarrow{\alpha\rho(s)x} f \tag{5}$$

This reaction corresponds mainly to the synthesis of proteins and nucleic acids, which depends on nitrogen availability. We therefore consider as in Ross and Geider (2009) that the synthesis rate is proportional to the nitrogen assimilation rate.

The sugar compartment g is also used in a parallel pathway to synthesize free fatty acids (FFA):

$$g \xrightarrow{\beta q_n \mu(q_n)x} \mathrm{FFA} \tag{6}$$

We assume that this rate of fatty acid synthesis depends on the photosynthesis rate $\mu(q_n)$, but that it is also modulated by the nitrogen quota. This assumption is based on the work of Sukenik and Livne (1991) who have explored the relationship between growth rate and lipid production in nitrogen limited cultures of *Isochrysis* aff. *galbana*.

These fatty acids are then mobilized to the production of functional carbon (mainly membranes):

$$\mathrm{FFA} \xrightarrow{\gamma\rho(s)x} f \tag{7}$$

The rate of this reaction is assumed to be proportional to the synthesis of proteins and nucleic acids (reaction (5)).

Finally, as free fatty acids are not stored in the cell (Ohlrogge and Browse, 1995; Guschina and Harwood, 2009), neutral lipids (i.e. mainly triglycerides) are used to store or to provide fatty acids when there is a disequilibrium between fatty acid synthesis (reaction (6)) and mobilization (reaction (7)):

$$\mathrm{FFA} \leftrightarrow l \tag{8}$$

We assume that this reaction rate is fast enough compared to the other reactions to maintain a constant FFA quota. Moreover, we consider that FFA pool is of negligible size (Ohlrogge and Browse, 1995; Guschina and Harwood, 2009) so that the model does not describe its dynamic.

A representation of the carbon flows is given in Fig. 2a. This scheme can be simplified (see Fig. 2b) assuming a low and constant FFA quota.

Assuming that the main mass transfer of carbon and nitrogen can be summarized by the reactions (1)–(8), the time-varying evolution equations resulting from mass balances considerations (Bastin and Dochain, 1990) in a homogeneous photobioreactor are given by:

$$\begin{cases} \dot{s} = Ds_{in} - \rho(s)x - Ds \\ \dot{n} = \rho(s)x - Dn \\ \dot{g} = (1-\beta q_n)\mu(q_n)x - \alpha\rho(s)x - Dg \\ \dot{l} = \beta q_n \mu(q_n)x - \gamma\rho(s)x - Dl \\ \dot{f} = (\alpha+\gamma)\rho(s)x - Df \end{cases} \tag{9}$$

where D is the dilution rate (ratio of the influent flow rate over the photobioreactor volume) and s_{in} the influent nitrate concentration.

From Eq. (9) we can deduce the dynamics of the nitrogen quota q_n, the carbon biomass which is the sum of the three carbon pools $x = f + g + l$, and the quotas of neutral lipid $q_l = l/x$ and functional carbon $q_f = f/x$, leading to the following set of equations:

$$\begin{cases} \dot{s} = Ds_{in} - \rho(s)x - Ds \\ \dot{q}_n = \rho(s) - \mu(q_n)q_n \\ \dot{x} = \mu(q_n)x - Dx \\ \dot{q}_l = (\beta q_n - q_l)\mu(q_n) - \gamma\rho(s) \\ \dot{q}_f = -q_f\mu(q_n) + (\alpha+\gamma)\rho(s) \end{cases} \tag{10}$$

It is worth noting that the first three equations of system (10) are *exactly* the Droop model (Droop, 1968, 1983). This model presents the advantage of being simple and having been extensively studied and validated (Droop, 1983; Sciandra and Ramani, 1994; Bernard and Gouzé, 1999). Moreover, the system has a cascade structure: the dynamics of the fractions q_l and q_f are not involved in the first three equations.

3. Model calibration

3.1. Parameter value computation

First, we present some model properties that will be used to identify the parameter values. In the Droop model, it can be proved (see Bernard and Gouzé, 1995) that the nitrogen quota stays between two bounds:

$$Q_0 \leqslant q_n \leqslant Q_m \tag{11}$$

with

$$Q_m = Q_0 + \frac{\rho_m}{\bar{\mu}} \tag{12}$$

Q_m represents the maximum cell quota obtained in conditions of non limiting nutrients, and the minimum quota, Q_0, is obtained in batch conditions after limiting nutrient depletion. Thus, we can deduce a maximal growth rate μ_m:

$$\mu_m = \mu(Q_m) = \bar{\mu}\left(1 - \frac{Q_0}{Q_m}\right) \tag{13}$$

This property will be used to compute $\bar{\mu}$, from the minimal and maximal nitrogen quota Q_0 and Q_m:

$$\bar{\mu} = \mu_m \frac{Q_m}{Q_m - Q_0} \tag{14}$$

In order to simplify steady state computation for the quotas of neutral lipid q_l^* and functional carbon q_f^*, the dynamics of q_l and q_f in (10) can be rewritten:

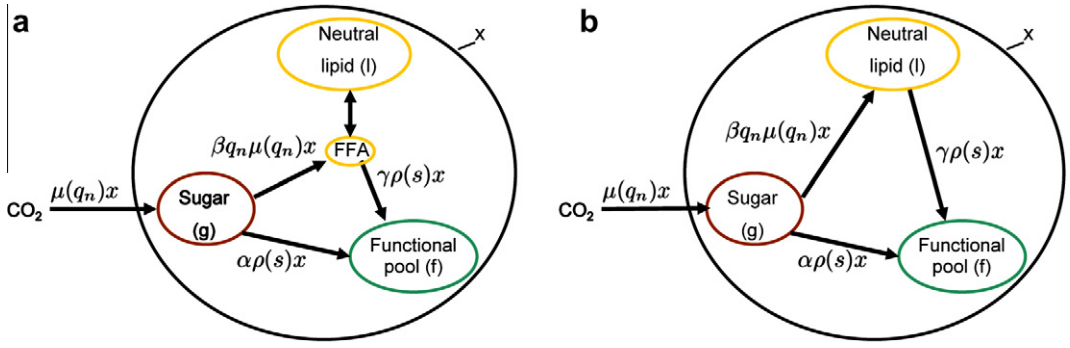

Fig. 2. (a) Representation of the carbon flows. The dynamics of neutral lipids result from the unbalance between fatty acid synthesis and mobilization. (b) Model simplification assuming that the quota of free fatty acids is very low and almost constant.

$$\begin{cases} \dot{q}_l = [(\beta-\gamma)q_n - q_l]\mu(q_n) - \gamma\dot{q}_n \\ \dot{q}_f = [(\alpha+\gamma)q_n - q_f]\mu(q_n) + (\alpha+\gamma)\dot{q}_n \end{cases} \quad (15)$$

At steady state, as $\dot{q}_n = 0$, we obtain the following equilibrium:

$$\begin{cases} q_l^* = (\beta-\gamma)q_n^* \\ q_f^* = (\alpha+\gamma)q_n^* \end{cases} \quad (16)$$

The model predicts thus, at steady state, that neutral lipid and functional carbon quotas are proportional to the nitrogen quota. Steady state of the sugar quota q_g^* is deduced from the relation $q_l + q_f + q_g = 1$:

$$q_g^* = 1 - (\beta+\alpha)q_n^* \quad (17)$$

As both $q_l^*(q_n)$ and $q_f^*(q_n)$ are linear increasing functions, $q_g^*(q_n)$ is a linear decreasing function.

Parameters α, β and γ can then be computed from the previous equations, using quota measurements at steady state.

3.2. Parameter estimation

The model is calibrated using the first part of the experiment (from the beginning to day 18), the remaining set of data is kept in order to further evaluate the validity of the model. We uncouple the estimation into two groups of parameters: the Droop parameters ($Q_0, \bar{\mu}, \rho_m, K_s$) and the intracellular carbon flow parameters ($\alpha, \beta,$ and γ). The Droop parameters can be easily determined, on the basis of dedicated experimental conditions, and then, the carbon parameters are identified.

The minimal nitrogen quota Q_0 is obtained from the nitrogen quota measurement during a nitrogen starvation experiment (data not shown). The maximum nitrogen quota Q_m and specific growth rate μ_m are estimated directly from the nitrogen quota measurements and the dilution rate during the non-limited growth phase (at the beginning of the experiment, see Fig. 3). The maximal absorption rate ρ_m and growth parameter $\bar{\mu}$ are obtained with relations (12) and (14). The half-saturation constant K_s is taken from previous experiments (data not shown).

The second step of the calibration procedure concerns the intracellular carbon flow parameters. The data obtained at steady state for two dilution rates (at days 2 and 17) are used to determine, thanks to Eq. (16), the parameters α, β, and γ: using an estimation of the slopes of $q_l^*(q_n)$ and $q_f^*(q_n)$ lines, we obtain a system of two equations with three unknown parameters. This system is used to calibrate the model with only one degree of freedom and thus obtain a first estimate of these parameters. Finally, the Levenberg–Marquardt minimization algorithm (function lsqcurvefit under Matlab®) initialised with these values is used as a final adjustment between model simulation and experimental data (from the beginning to day 18). Calibration results are given in Table 1.

4. Results and discussion

4.1. Model simulation

The model was simulated and results were compared with experimental data of a *Isochrysis* aff. *galbana* culture, with various nitrogen limitations. The second part of the experiment (from day 18 to the end) was used in order to validate the model with experimental data not used for model calibration. Results shown in Fig. 3 demonstrate that the model predicts quite accurately the dynamics of nitrate concentration s, nitrogen quota q_n and biomass x. This corroborates the fact that the Droop model has been widely validated (Droop, 1983; Sciandra and Ramani, 1994; Bernard and Gouzé, 1999) for its aptitude to predict both biomass and remaining inorganic nitrogen. The low nitrogen quota for most

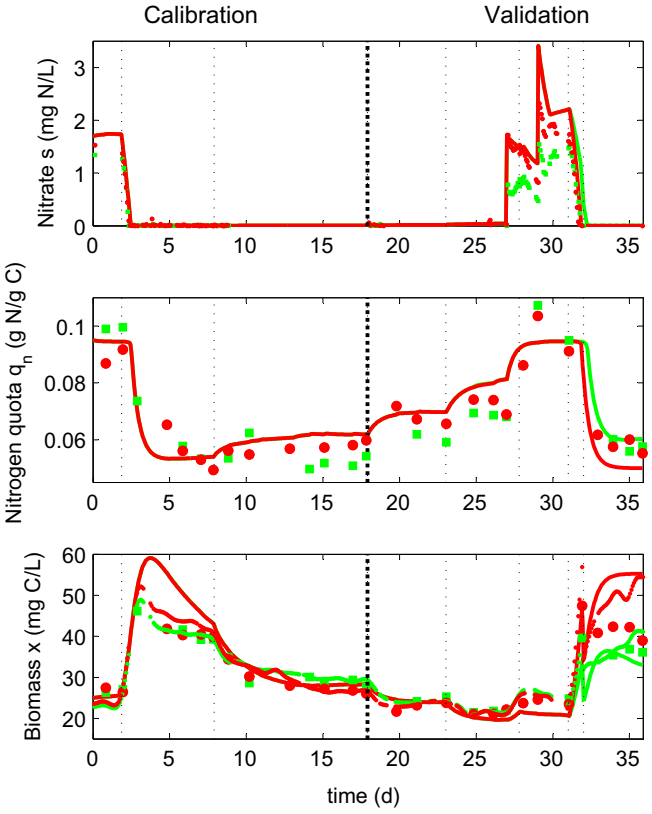

Fig. 3. Comparison of the Droop model (lines) with the data (symbols) of *Isochrysis* aff. *galbana* culture under various nitrogen conditions. Red lines and circles: photobioreactor A (ended by a nitrogen starvation) and green lines and squares: photobioreactor B (ended by a nitrogen limitation). Carbon biomass is measured (circles and squares) and deduced from biovolume measurements (dots). Vertical lines indicate dilution rate changes. (For interpretation of the references to colour in this figure legend, the reader is referred to the web version of this article.)

Table 1
Parameters obtained by the calibration of the model.

Parameter	Value
Minimal nitrogen quota, Q_0	0.05 mg[N] mg[C]$^{-1}$
Maximal nitrogen quota, Q_m	0.095 mg[N] mg[C]$^{-1}$
Maximal growth rate, μ_m	1 d^{-1}
Protein synthesis coefficient, α	2.6 mg[C] mg[N]$^{-1}$
Fatty acid synthesis coefficient, β	4.8 mg[C] mg[N]$^{-1}$
Fatty acid mobilization coefficient, γ	3.0 mg[C] mg[N]$^{-1}$
Half-saturation constant, K_s	0.018 mg[N] L^{-1}
Theoretical maximum growth rate, $\bar{\mu}$[a]	2.11 d^{-1}
Maximal uptake rate, ρ_ma	0.095 mg[N] mg[C]$^{-1}$ d^{-1}

[a] Parameters computed from Q_0, Q_m and μ_m.

of the experiment confirms that the cells are nitrogen limited, and that several levels of limitation are experimented, ranging from starvation to repletion. The simulated and experimental distributions of intracellular carbon between sugars, neutral lipids and functional pool are presented in Fig. 4. The model accurately predicts the behaviour of the carbon quotas during all the experiment, in spite of the fact that it has been calibrated only with the first part of the experiment. Moreover, the evolution of the distribution of intracellular carbon is well described both in steady states and in dynamic conditions.

4.2. Steady states

We can also analyse the behaviour of the model in order to explain the complex dynamics of the distribution of intracellular

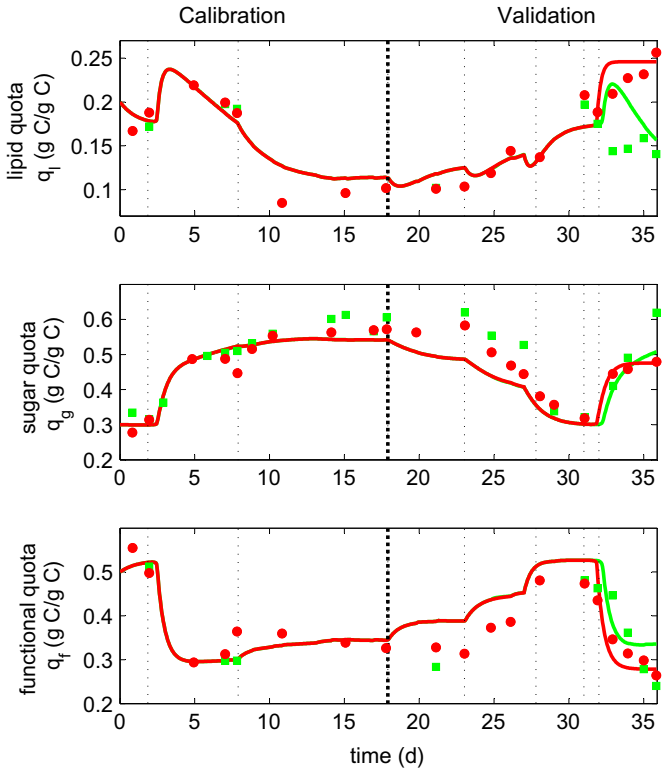

Fig. 4. Comparison of the predicted neutral lipid and sugar quotas (lines) with experimental data (symbols) of *Isochrysis* aff. *galbana* culture under various nitrogen limitation rates. Red lines and circles: photobioreactor A (ended by a nitrogen starvation) and green lines and squares: photobioreactor B (ended by a nitrogen limitation). Vertical lines indicate dilution rate changes. (For interpretation of the references to colour in this figure legend, the reader is referred to the web version of this article.)

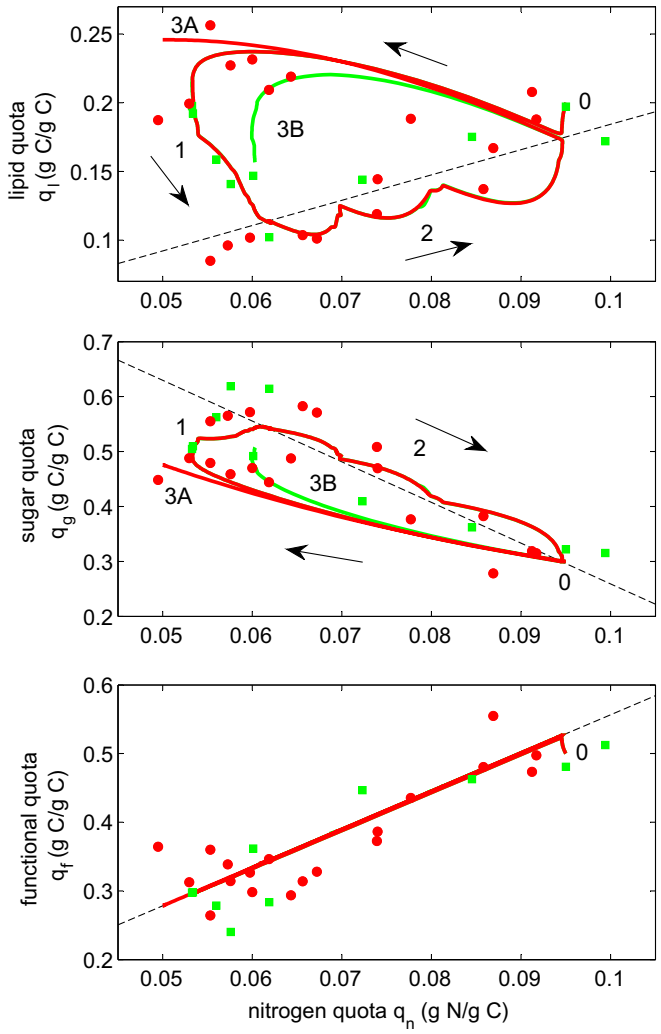

Fig. 5. Hysteretic behaviour of neutral lipid and sugar quotas as a function of nitrogen quota: comparison of model (lines) and experimental data (symbols). Red lines and circles: photobioreactor A (ended by a nitrogen starvation); green lines and squares: photobioreactor B (ended by a nitrogen limitation); and dashed line: model equilibrium. Numbers and arrows indicate the chronological sequence: (1) nitrogen limitation, (2) decrease of the nitrogen stress, (3A) starvation or (3B) limitation. (For interpretation of the references to colour in this figure legend, the reader is referred to the web version of this article.)

carbon. In stabilized culture, Eqs. (16) and (17) show that the quotas of neutral lipid, sugar and functional carbon are linearly correlated to the nitrogen quota. This result is validated with the experimental data obtained at steady states in chemostats run at various dilution rates (see Fig. 5). Therefore, a high nitrogen quota leads at equilibrium to a high neutral lipid quota and a low sugar quota.

4.3. Model reduction

Let us assume that we start at t_0 from a steady state condition. Let us denote $\delta = (\alpha+\gamma)q_n - q_f$. From Eq. (16), we get $\delta(t_0) = 0$. Moreover, using Eq. (15) we have $\dot{\delta} = -\delta\mu(q_n)$. As a consequence, $\delta(t) = 0$ for $t \geqslant t_0$, and thus:

$$q_f(t) = (\alpha+\gamma)q_n(t) \tag{18}$$

Therefore, the functional quota is proportional to the nitrogen quota. This correlation is validated by experimental data on Fig. 5. Thus, equation $\dot{q}_f$ of the model (10) can be removed and substituted by Eq. (18). Note that this correlation is also obtained in Ross and Geider (2009). These authors consider that cellular nitrogen is contained only in the functional pool which has a fixed N:C ratio, explaining thus the correlation between nitrogen and functional quotas.

4.4. Hysteresis behaviour

Let us consider a situation where the cells are in a steady state characterized by a high nitrogen content q^*_{n1}. If the dilution rate is decreased, the cells undergo a decrease of their nitrogen quota down to a value $q^*_{n2} < q^*_{n1}$. This means that, during this transient, we have $\dot{q}_n < 0$ (Bernard and Gouzé, 1995). We consider variable $z = q_l - (\beta-\gamma)q_n$ representing the distance between the lipid quota and its equilibrium value . Using Eq. (15) for $\dot{q}_l$, the dynamics of z are:

$$\dot{z} = -z\mu(q_n) - \beta\dot{q}_n \tag{19}$$

As z is initially null (steady state), z remains non-negative during this transient so that q_l stays above the equilibrium line of equation $q^*_l = (\beta-\gamma)q^*_n$. Once the nitrogen quota has reached its steady state value, we have $\dot{q}_n = 0$. It follows that z tends toward zero and q_l finally reaches its steady state on the line $q^*_l = (\beta-\gamma)q^*_n$.

Note that this behaviour is possible only since $\mu(q_n)$ is not zero, and is decreasing from $\mu(q_{n1})$ down to $\mu(q_{n2}) > 0$.

This transient behaviour of q_l is observed on Fig. 5 (phase 1).

The same reasoning can explain the behaviour of the lipid content, when the internal nitrogen quota is increased (following for example an increase in the dilution rate). In this case, we can show that q_l will increase but stay under the line $q^*_l = (\beta-\gamma)q^*_n$ (see

Fig. 5, phase 2) . This behaviour leads to a phenomenon of hysteresis: the trajectory between two steady states when nitrogen limitation is increasing is very different from the trajectory after a decrease in nitrogen limitation (see Fig. 5).

4.5. Nitrogen starvation

In case of nitrogen starvation (i.e. $s^* = 0$), q_n decreases from Q_m down to Q_0 (where growth stops). The lipid quota does not reach the equilibrium line but since growth stops, it reaches a steady state value $q_l^\dagger$ which can be computed as follows (see Appendix A for details):

$$q_l^\dagger = Q_0\left[(\beta-\gamma)+\beta\ln\left(\frac{Q_m}{Q_0}\right)\right] \tag{20}$$

If the parametric condition

$$\frac{\beta-\gamma}{\beta} < \frac{Q_0}{Q_m-Q_0}\ln\left(\frac{Q_m}{Q_0}\right) \tag{21}$$

is verified, expression (20) shows that the final lipid content after nitrogen exhaustion is greater than $(\beta-\gamma)Q_m$, the maximum amount of lipid reached in balanced growth. It means that lipid content is higher after nitrogen starvation, that at unlimited growth rate. With the computed parameters (Table 1), condition of Eq. (21) is fulfilled for *Isochrysis* aff. *galbana*. Nitrogen starvation at the end of the experiment in photobioreactor A confirms this result: the lipid content is increased during the batch phase where internal nitrogen quota reaches its minimal value. Nevertheless, the lipid content response to nitrogen starvation is known to be highly species dependent, and some species can reach higher lipid quota in nitrogen replete conditions compared to nitrogen starvation (Griffiths and Harrison, 2009). This means that the condition of Eq. (21) may not be satisfied for such species.

A comparison between nitrogen limitation (starting at day 2 and 31 in photobioreactor B) and nitrogen starvation (starting at day 31 in photobioreactor A) is of particular interest. The model predicts that such a protocol should lead to radically different behaviour of neutral lipid quota. For nitrogen limitation, a lower value of the lipid content should be reached after a transient increase, while the starvation should lead to an enhanced value of q_l, higher than the maximum obtained in balanced growth conditions. Fig. 4 and 5 show that these predictions are experimentally verified.

4.6. Behaviour of sugar quota

Using the same approach as in Section 4.4, we can show that, when the internal nitrogen quota is increased (resp. decreased), the sugar quota q_g will decrease over (resp. increase under) the equilibrium line $q_g^* = 1-(\beta+\alpha)q_n^*$. The experimental data in Fig. 5 validates this phenomenon of hysteresis for the sugar quota.

The sugar quota $q_g^\dagger$ obtained after nitrogen starvation can be computed from Eqs. (18) and (20):

$$q_g^\dagger = 1 - q_l^\dagger - (\alpha+\gamma)Q_0 \tag{22}$$

Note that a starvation and a limitation both lead to a sugar quota increase but the starvation gives a smaller quota than a limitation (see Fig. 5).

4.7. Neutral lipid accumulation

The proposed model, supported by the experimental results, can help in explaining the distribution of intracellular carbon. During nitrogen starvation, production of functional carbon (reactions (5) and (7)) is stopped so that the incoming carbon is stored in sugar and neutral lipid pools, leading to an increase of these quotas until growth stops (once the nitrogen quota has reached its minimum) (Thompson, 1996; Sobczuk and Chisti, 2010).

The distribution of intracellular carbon points towards a complex behaviour in response to other nitrogen conditions (see Fig. 4 and 5). The dynamic of neutral lipid quota is due to the imbalance between biomass growth (inducing intracellular dilution) and neutral lipid net production. Neutral lipid net production (reaction (8)) is itself the difference between fatty acid production (reaction (6)) and its mobilization (reaction (7)). It is generally accepted that microalgae produce more fatty acids than they need under non-stress conditions (Thompson, 1996) leading thus to the production of neutral lipids to store the excess.

From extensive simulations, it appears that neutral lipid net production predicted by the model is always positive except during the transient recovery from nitrogen starvation or limitation. This result is consistent with observations of Khozin-Goldberg et al. (2005) with *Parietochloris incisa* which show that neutral lipid are mobilized for the construction of chloroplastic membranes following recovery from nitrogen starvation. Livne and Sukenik (1992) have also suggested that the recovery of lipid synthesis rate was slower than division rate. Therefore, in such a case, neutral lipids are mobilized in order to compensate for the delay in the fatty acid productions and ensure rapid recovery of growth.

Note that neutral lipid utilization is also observed in response to a low-temperature induced stress (Cohen et al., 2000) or in darkness (Thompson, 1996). The light and temperature effects on growth and lipid accumulation are beyond the scope of this article but the model could be modified to take it into account.

4.8. Neutral lipid and sugar productivities

In a continuous culture, the steady states computed using Eq. (10) are defined by Eq. (16) and:

$$\begin{cases} q_n^* = \frac{\bar{\mu}Q_0}{\bar{\mu}-D} \\ s^* = \frac{K_s D q_n^*}{\rho_m - D q_n^*} \\ x^* = \frac{s_{in}-s^*}{q_n^*} \end{cases} \tag{23}$$

Biomass, sugar and neutral lipid productivities (denoted, respectively, P_x, P_g and P_l) in a continuous culture at equilibrium can be computed from model equations as follows:

$$\begin{cases} P_x = Dx^* \\ P_g = Dx^* q_g^* \\ P_l = Dx^* q_l^* \end{cases} \tag{24}$$

The model accurately predicts the experimental productivities in continuous culture (see Fig. 6). It can thus forecast the maximal neutral lipid productivity, obtained for a growth rate $\mu = 0.95\ \mathrm{d}^{-1}$, i.e. for 95% of the maximal growth rate. The productivity trade-off is then mainly driven by the growth rate. The maximal sugar productivity is obtained for a growth rate $\mu = 0.66\ \mathrm{d}^{-1}$, i.e. for 66% of the maximal growth rate. In that case, the corresponding trade-off is more influenced by carbohydrate accumulation. As this work is focused on lipid kinetics in relation to nitrogen status, only diluted cultures have been considered in order to avoid any experimental bias due to light change or light gradient. The prediction of maximal reachable productivities for high density culture should then also include modelling of growth in the light gradient, involving radiative transfer modelling (Pruvost et al., 2009).

This steady state analysis for a continuous process can, however, not straightforwardly be compared to the productivity obtained in batch. In such a case, the previous scenario of continuous production must be compared to a scenario of two stage batch production, with a first phase of biomass growth and

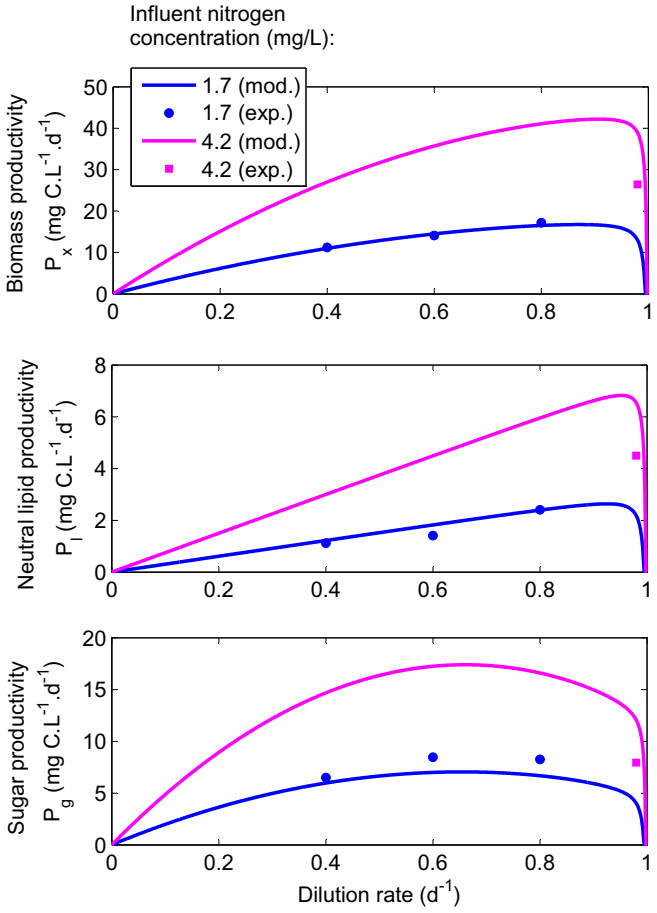

Fig. 6. Biomass, neutral lipid and sugar productivities: comparison of model (lines) and experimental data (symbols) with influent nitrogen concentration $s_{in} = 1.7$ mg/L (in blue) and $s_{in} = 4.2$ mg/L (in magenta). (For interpretation of the references to colour in this figure legend, the reader is referred to the web version of this article.)

a second phase of nitrate exhaustion and nitrogen starvation, as proposed by Huntley and Redalje (2007). From a theoretical point of view, this is a complex and challenging optimal control problem with non-linear dynamics. However, to solve such a problem, light intensity must also be taken into account in the model, and a radiative transfer model must be associated to predict the light gradient. Only the outcome of these two models can predict productivity in realistic large-scale production, i.e. under natural irradiance and light limitation. Currently, insufficiently rigorous experimental data limit comparison of these two possible working modes (Griffiths and Harrison, 2009). Finally, a combination of these two working modes may be the optimal solution: a biomass production in continuous culture followed by a batch starvation in order to increase the neutral lipid content (Sobczuk and Chisti, 2010).

5. Conclusions

We have presented a model for neutral lipid production by microalgae. Its strength is to predict accurately both the steady state and the transient phases in various physiological conditions from low nitrogen limitation to starvation. The model, based on the Droop approach, has a minimal degree of complexity so that it can be mathematically analysed. It highlights and explains the hysteresis phenomenon in neutral lipid production which has been experimentally verified: the lipid dynamics after nitrogen starvation is highly different from the dynamics after nitrogen recovery. The model must be assessed and validated with other microalgal species. Coupled with a model of light distribution, it will then be used to predict and optimize lipid production in the perspective of large-scale biofuel production.

Acknowledgement

This paper presents research results supported by the ANR-06-BIOE-014 Shamash project.

Appendix A. Computation of final lipid quota after nitrogen starvation

The dynamics of q_n and q_l, once external nitrate have been exhausted are:

$$\begin{cases} \dot{q}_n = -\mu(q_n)q_n \\ \dot{q}_l = (\beta q_n - q_l)\mu(q_n) \end{cases} \tag{25}$$

Using these equations, the dynamic of $v = \frac{q_l}{q_n}$ is:

$$\dot{v} = \frac{q_n\dot{q}_l - q_l\dot{q}_n}{q_n^2} = -\frac{\beta}{q_n}\dot{q}_n \tag{26}$$

Integrating from t_1 to t_2, we obtain:

$$v_2 - v_1 = \int_{t_1}^{t_2} \dot{v}\,dt = \int_{q_{n1}}^{q_{n2}} -\frac{\beta}{q_n}dq = [-\beta \ln q_n]_{q_{n1}}^{q_{n2}} \tag{27}$$

Now consider a complete starvation from a non-limited equilibrium, i.e. $q_{n1} = Q_m, q_{l1} = (\beta - \gamma)Q_m, q_{n2} = Q_0$ and $q_{l2} = q_l^\dagger$, the last expression becomes:

$$\frac{q_l^\dagger}{Q_0} - \frac{(\beta-\gamma)Q_m}{Q_m} = [-\beta \ln q_n]_{Q_m}^{Q_0} = \beta \ln \frac{Q_m}{Q_0} \tag{28}$$

From this equation, we can deduce the expression of $q_l^\dagger$.

References

Bastin, G., Dochain, D., 1990. On-line Estimation and Adaptive Control of Bioreactors. Elsevier, New York.
Bernard, O., Gouzé, J.L., 1995. Transient behavior of biological loop models, with application to the Droop model. Math. Biosci. 127 (1), 19–43.
Bernard, O., Gouzé, J.-L., 1999. Nonlinear qualitative signal processing for biological systems: application to the algal growth in bioreactors. Math. Biosci. 157, 357–372.
Bernard, O., Queinnec, I., 2008. Dynamic models of biochemical processes: properties of models. In: Dochain, D. (Ed.), Bioprocess Control. Wiley, Hoboken (Chapter 2).
Bligh, E., Dyer, W., 1959. A rapid method of total lipid extraction and purification. Canad. J. Biochem. Physiol. 37, 911–917.
Chisti, Y., 2007. Biodiesel from microalgae. Biotechnol. Adv. 25, 294–306.
Cohen, Z., Khozin-Goldberg, I., Adlerstein, D., Bigogno, C., 2000. The role of triacylglycerol as a reservoir of polyunsaturated fatty acids for the rapid production of chloroplastic lipids in certain microalgae. Biochem. Soc. Trans. 28, 740–743.
Droop, M.R., 1968. Vitamin B12 and marine ecology. IV. The kinetics of uptake growth and inhibition in *Monochrysis lutheri*. J. Mar. Biol. Assoc. 48 (3), 689–733.
Droop, M.R., 1983. 25 years of algal growth kinetics, a personal view. Botan. Marina 16, 99–112.
Dubois, M., Gilles, K., Hamilton, J., Rebers, P., Smith, F., 1956. Colorimetric method for determination of sugars and related substances. Anal. Chem. 28, 350–356.
Falkowski, P.G., Raven, J.A., 2007. Aquatic Photosynthesis. Princeton University Press, Princeton.
Faugeras, B., Bernard, O., Sciandra, A., Levy, M., 2004. A mechanistic modelling and data assimilation approach to estimate the carbon/chlorophyll and carbon/nitrogen ratios in a coupled hydrodynamical-biological model. Nonlinear Process. Geophys. 11, 515–533.
Geider, R., MacIntyre, H., Kana, T., 1998. A dynamic regulatory model of phytoplanktonic acclimation to light, nutrients, and temperature. Limnol. Oceanogr. 43, 679–694.
Geider, R.J., Roche, J.L., 2002. Redfield revisited: variability of C:N:P in marine microalgae and its biochemical basis. Eur. J. Phycol. 37, 1–17.
Griffiths, M.J., Harrison, S.T.L., 2009. Lipid productivity as a key characteristic for choosing algal species for biodiesel production. J. Appl. Phycol. 21, 493–507.

Guschina, I., Harwood, J., 2009. Algal Lipids and Effect of the Environment on their Biochemistry. Springer, New York.
Hsieh, C.-H., Wu, W.-T., 2009. Cultivation of microalgae for oil production with a cultivation strategy of urea limitation. Bioresour. Technol. 100, 3921–3926.
Huntley, M., Redalje, D., 2007. CO_2 mitigation et renewable oil from photosynthetic microbes: a new appraisal. Mitigat. Adaptat. Strat. Global Change 12, 573–608.
Khozin-Goldberg, I., Shrestha, P., Cohen, Z., 2005. Mobilization of arachidonyl moieties from triacylglycerols into chloroplastic lipids following recovery from nitrogen starvation of the microalga *Parietochloris incisa*. Biochim. Biophys. Acta 1738, 63–71.
Le Floc'h, E., Malara, G., Sciandra, A., 2002. An automatic device for in vivo absorption spectra acquisition in phytoplanktonic cultures: application to the study of photoadaptation to light and nutrient variations. J. Appl. Phycol. 14, 435–444.
Livne, A., Sukenik, A., 1992. Lipid synthesis and abundance of acetyl Coa carboxylase in *Isochrysis galbana (Prymnesiophyceae) following nitrogen starvation*. Plant Cell Physiol. 33, 1175–1181.
Lv, J.-M., Cheng, L.-H., Xu, X.-H., Zhang, L., Chen, H.-L., 2010. Enhanced lipid production of *Chlorella vulgaris* by adjustment of cultivation conditions. Bioresour. Technol. 101, 6797–6804.
Metting, F., 1996. Biodiversity and application of microalgae. J. Indust. Microbiol. Biotechnol. 17, 477–489.
Ohlrogge, J., Browse, J., 1995. Lipid biosynthesis. Plant Cell 7, 957–9708.
Pahlow, M., 2005. Linking chlorophyll nutrient dynamics to the Redfield N:C ratio with a model of optimal phytoplankton growth. Mar. Ecol. Prog. Ser. 287, 33–43.
Pruvost, J., Vooren, G.V., Cogne, G., Legrand, J., 2009. Investigation of biomass and lipids production with *Neochloris oleoabundans* in photobioreactor. Bioresour. Technol. 100, 5988–5995.
Rodolfi, L., Zittelli, G.C., Bassi, N., Padovani, G., Biondi, N., Bonini, G., Tredici, M.R., 2009. Microalgae for oil: strain selection, induction of lipid synthesis and outdoor mass cultivation in a low-cost photobioreactor. Biotechnol. Bioeng. 102 (1), 100–112.
Ross, O., Geider, R., 2009. New cell-based model of photosynthesis and photo-acclimation: accumulation and mobilisation of energy reserves in phytoplankton. Mar. Ecol. Prog. Ser. 383, 53–71.
Sciandra, A., Ramani, P., 1994. The limitations of continuous cultures with low rates of medium renewal per cell. J. Exp. Mar. Biol. Ecol. 178, 1–15.
Sobczuk, T., Chisti, Y., 2010. Potential fuel oils from the microalga *Choricystis minor*. J. Chem. Technol. Biotechnol. 85, 100–108.
Sukenik, A., Livne, A., 1991. Variations in lipid and fatty acid content in relation to acetyl CoA carboxylase in the marine Prymnesiophyte *Isochrysis galbana*. Plant Cell Physiol. 32, 371–378.
Thompson Jr., G.A., 1996. Lipids and membrane function in green algae. Biochim. Biophys. Acta 1302, 17–45.